Int j simul model 15 (2016) 4, 688-698
ISSN 1726-4529 Original scientific paper

SIMULATION OF NON-OVERLOAD CHARACTERISTICS OF SERIAL-PARALLEL CENTRIFUGAL PUMPS

Li, Q.[*]; Yan, H.[*]; Shi, H. X.[*]; Han, X. X.[*] & He, H. Y.[**]
[*] Research Institute of Chemical Machinery, Hefei University of Technology, Tunxi Road No.193, Hefei, P. R. China
[**] School of Computing Science, Newcastle University, NE1 7RU, United Kingdom
E-Mail: yanying0708@126.com

Abstract
Serial-parallel centrifugal pumps (SPCPs) are a new type of pump with two working conditions: high head with low flow and low head with high flow. However, the motor of SPCPs is easily burned because of its various operating conditions. To clarify the effect of the flow field on the non-overload characteristics of SPCPs, revealing the non-uniformity of the flow distribution is necessary. This study derived the velocity triangle theory of the pump, and a numerical simulation by 3D models was conducted to investigate the internal flow patterns of SPCPs. The magnitude of the flow deviation angle at different cross-sections was calculated to evaluate the non-overload characteristics under different operating conditions. The results showed that the formula of the maximum shaft power and the local flow rate were two important parameters of the non-overload interpretation of the pump. The simulated results were in good agreement with the experimental results at the designed flow rate. In addition, the flow deviation angle under the serial operating condition, which was more likely to achieve the non-overload characteristics, was evidently higher than that under the parallel operating condition. The conclusions solved the issue on the theoretical design of the non-overload characteristics considered in a non-uniform flow in SPCPs.
(Received in April 2016, accepted in June 2016. This paper was with the authors 1 month for 1 revision.)

Key Words: Serial-Parallel Centrifugal Pumps, Non-Overload Characteristics, Numerical Simulation, Parametric Modelling, Flow Deviation Angles

1. INTRODUCTION

Serial-Parallel Centrifugal Pumps (SPCPs) are widely used in shipping industry and fire protection field, since they have compact structure and low cost [1]. However, the shaft power curves of them are mounting steeply with the increase of the flow rate [2-5], which will bring about the motor surcharge form damaging at the lager flow rate, since they have various operating conditions. For hydraulic machinery, it's particularly important that the motors are not burnt-out when operating under all conditions, which means there is a maximum value on the flow and power curves meeting the requirements of the actual flow. This nature is also the non-overload characteristic of pumps.

A number of factors affect the non-overload performance of SPCPs, and the non-uniformity of flows is one of the key factors. The effect of swirling flows, secondary refluxes, and flow separation can be normally ignored under the design rate of the general centrifugal pump. However, for the multi-stage pumps and SPCPs, which have complex internal passages, the effects of non-uniform flows on the performance cannot be neglected [6]. Moreover, the adverse flows appear when the pumps work under the design rate. These non-uniform flows greatly affect the safety of the pumping systems, especially the phenomenon of the motor burnout when working overload. Therefore, lengthening the time of use is important so that the power of hydraulic pumps is optimized to meet the non-overload performance requirements.

2. STATE OF THE ART

SPCPs are a new type of pump that can achieve two operating conditions by adjusting the reversing valves. The two operating conditions are the serial operating condition and the parallel operating condition.

Yu et al. [7] described the characteristics, structure, and hydraulic design of a marine submersible SPCP. The submersible ship SPCP of 200CBLQ-13 was designed according to the requirements of marine applications. Li et al. [8, 9] optimized the structure of the SPCP, tested the external characteristic and vibration, and compared and analysed the vibration characteristic and the different structures of the pump. Yu et al. and Li et al. studied the non-overload characteristics of pumps.

Currently, only a few studies have attempted to perform an experimental validation of the numerical results using the computational fluid dynamics (CFD) to measure the flow pattern in hydraulic machinery. Further research shows that the CFD widely deals with the non-overload performance of pumps. Anderson proposed area ratio theory [10, 11], which states that the shaft power of centrifugal pumps reaches the maximum with a theoretical head of $u_2^2/2g$. Yuan [12] and Zhang et al. [13] used the orthogonal experiment method to obtain data from external characteristic experiments of the impeller with different design parameters. The obtained data are an important reference value in designing a highly efficient and non-overload centrifugal pump. However, the orthogonal experiment method is time consuming, labour intensive, and costly. Feng et al. [14] adopted a simulation of a low-specific-speed radial diffuser pump to calculate periodically unsteady flow fields. The suitability of the proposed method is verified by the model tests according to the simulation results, and these tests enable the analysis of the non-overload characteristics of centrifugal pumps. Zhang et al. [15] used non-overload theory in combination with the orthogonal experiment to design splitters in low-specific-speed centrifugal pumps. The designed method was concluded to be reasonable and able to obtain the highly efficient and non-overload properties of pumps. Hu et al. [16] employed the maximum flow design method and the non-overload pump design method to derive the theory of non-overload operating conditions. The experimental data proved to be effective and reliable in improving the performance of a non-overload pump. However, the analysis of the non-overload hydraulic performance under uniform flow conditions did not present the non-uniformity of the flow pattern at the impeller inlet or impeller exit; thus, the precise prediction of the non-overload characteristics was hardly achieved. In the present paper, the computational equations of the non-overload characteristics, which consider the non-uniformity of the flow pattern, are derived on the basis of velocity triangle theory. Moreover, the flow deviation angle is introduced to describe them. The effect of the internal non-uniform flows on the non-overload characteristics of SPCPs using the combination of numerical simulation and experiment is discussed.

The remainder of this paper is organized as follows: Section 3 describes the physical model, the theoretical analysis of the non-overload characteristics, the calculation method, and the grid division of the calculation simulation. Section 4 presents the experiment results and discussion to validate the application of the numerical simulation method to simulate the flow field of pumps. The analysis of the distribution of non-uniform flow deviation angles and the effect of the angles on the non-overload characteristics of pumps is also presented. The conclusions are summarized in Section 5.

3. METHODOLOGY

3.1 Physical model

The physical model of SPCPs is illustrated in Fig. 1. SPCPs under the parallel operation

condition with a flow rate Q_P = 0.044 m³/s, head H_P = 80 m, and rotation speed n = 2980 r/min as well as SPCPs under the serial operation condition with flow rate Q_S = 0.022 m³/s, head H_S = 160 m, and rotation speed n = 49.667 r/s are investigated. The single-stage model pump (SSMP) of SPCPs with flow rate Q = 0.022 m³/s, head H = 80 m, and rotation speed n = 49.667 r/min is also designed.

The structure in Fig. 1 a, which is the same as that in reference [1], shows that the pumps take the serial operating condition when the top of the reversing valve remains in position C. However, when the top of the reversing valve remains in position D, the pumps are in the parallel operating condition. Fig. 1 b shows the hydraulic diagram of the half-helix suction chamber.

The specific speed of a single-stage pump is 16.608, which is equal to the example in deriving the energy equations of pumps. The impeller has six 3D (non-twisted) blades with an inlet and an exit diameter D_1 = 0.102 m and D_2 = 0.255 m, respectively, exit width b_2 = 0.01 m, and inlet angle of blade and exit angle of blade β_1 = 26° and β_2 = 49°, respectively. The blade shape is a simple circular arc with a constant thickness of 0.005 m, with both ends rounded (Fig. 1 c). The geometric parameters of the impellers and volutes of SPCP are the same as those of SSMP, and the connecting pipes of the hydraulic components of SPCP are uniformly transited using the area ratio method.

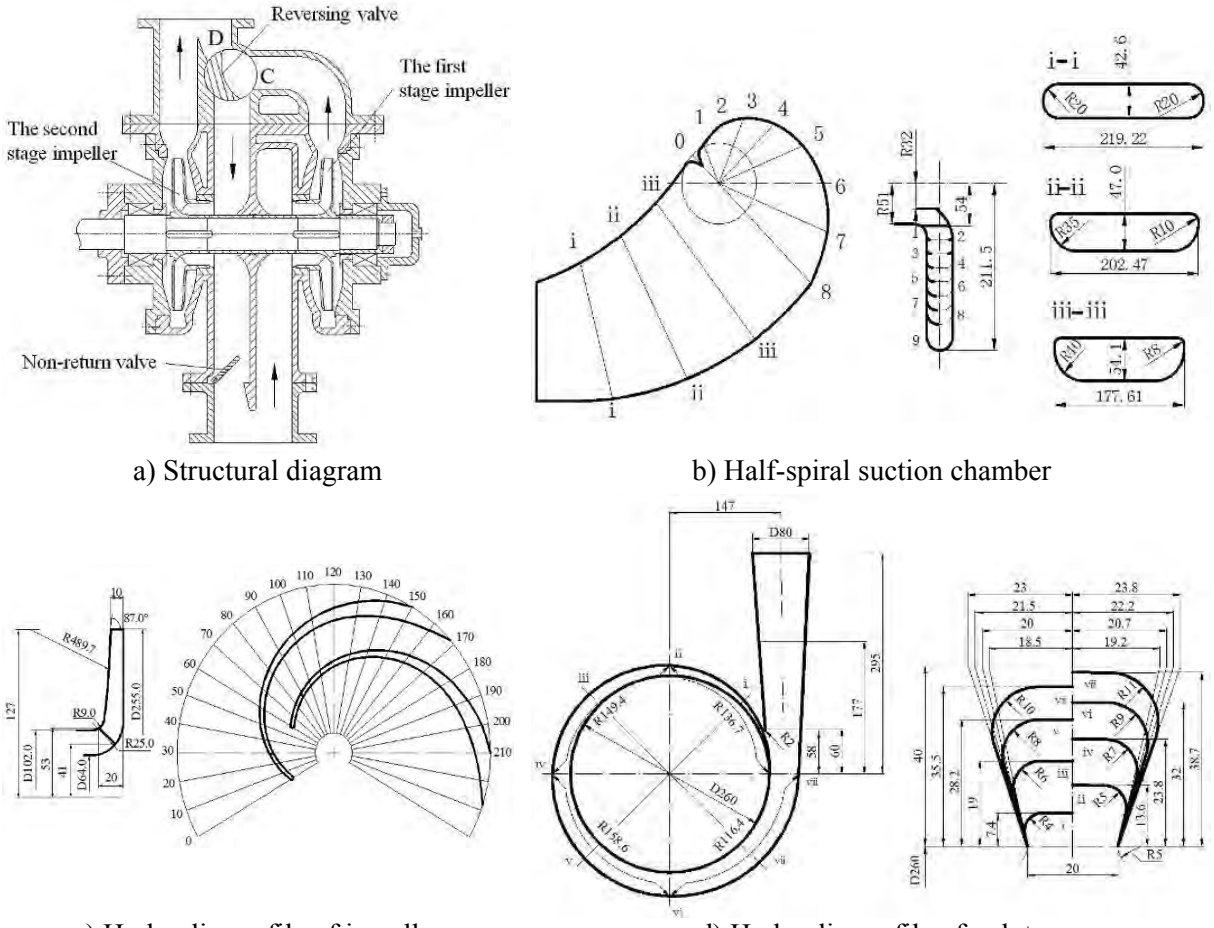

a) Structural diagram b) Half-spiral suction chamber

c) Hydraulic profile of impeller d) Hydraulic profile of volute

Figure 1: Schematic diagram and physical model of a series-parallel centrifugal pump.

3.2 Non-overload characteristics

The inlet and exit velocity triangles of impeller are shown in Fig. 2.

a) Inlet velocity triangle b) Exit velocity triangle

Figure 2: Velocity triangle of pump.

The velocity vector can be replaced by the mean velocity in the analysis of non-overload characteristics, and the tangential component of the absolute velocity of the impeller is written as follows:

$$v'_{u1} = v_{m1} \tan \gamma_1 \tag{1}$$

At the exit of the impeller, the non-uniform flow pattern shows some velocity-slip phenomenon. The exit tangential component of the absolute velocity of the impeller can be obtained as follows:

$$v'_{u2} = u_2 - v_{m2} \cot(\beta_2 - \gamma_2) \tag{2}$$

where, γ_2 is the deviation angle between the flow angle and the blade angle, and the exit axial velocity of blades can be written as:

$$v_{m2} = \frac{Q_t}{\pi D_2 b_2 \psi_2} \tag{3}$$

where, Q_t is theoretical flow rate, and ψ_2 is the exit excretion coefficient of the blades.

According to Euler equations, the energy equation of the pump under the uniform flow condition is defined as:

$$H_t = \frac{1}{g}(u_2 v_{u2} - u_1 v_{u1}) \tag{4}$$

where, $u_2 = \frac{\pi n D_2}{60}$, $u_1 = \frac{\pi n D_1}{60}$. Based on Eqs. (1)-(4), the energy equation of the non-uniform flow condition can be calculated as follows:

$$H_t = \frac{1}{g}\left(u_2 v'_{u2} - u_1 v'_{u1}\right) = \frac{1}{g}\left(u_2^2 - \left(\frac{n\cot\left(\beta_2 - \gamma_2\right)}{60 b_2 \psi_2} + \frac{n D_1 \tan \gamma_1}{15\left(D_1^2 - D_h^2\right)\ \psi_1}\right) Q_t\right) \tag{5}$$

The shaft power P can be computed from the following relation:

$$P = \frac{\rho u_2^2}{1000 \eta_m} Q_t - \left(\frac{\rho n \cot(\beta_2 - \gamma_2)}{60 \eta_m b_2 \psi_2} + \frac{\rho n D_1 \tan \gamma_1}{15 \eta_m (D_1^2 - D_h^2) \psi_1}\right) \frac{Q_t^2}{1000} \tag{6}$$

The η_m is the mechanical efficiency. Eqs. (5) and (6) show that the energy equation and the shaft power equation are related to the flow deviation angle γ_i, where $\gamma_1 < 90°$ and $\gamma_2 < 45°$. Therefore, when the γ_i value is not equal to zero, the continuous flow is non-uniform, thereby causing a decrease in the head and shaft power. Thus, the non-uniform flow affects the characteristics of SPCPs.

In the volute, the designed geometric parameters also affect the hydraulic performance of pumps. One of the parameters shown in Fig. 1 d, the throat flow cross-sectional area (viii cross-sectional area), is directly related to the hydraulic performance of pumps. In this paper, the viii cross-sectional area proposed by Guan is used to design the present volute, which has a good flow condition that can perfectly match with the non-overload characteristics of pumps. Therefore, the effect of the two volutes on the non-overload characteristics of SPCPs can be neglected.

In Eq. (6), defining $A=\frac{\rho u_2^2}{\eta_m}$, $B=\frac{\rho n\cot(\beta_2-\gamma_2)}{60\eta_m b_2\psi_2}+\frac{\rho n D_1\tan\gamma_1}{15\eta_m(D_1^2-D_h^2)\psi_1}$, the Eq. (6) can be rewritten as $P=\frac{AQ_t-BQ_t^2}{1000}$.

Defining $\partial P/\partial Q_t=0$, the flow rate can be computed from the following relation:

$$Q_t=\frac{A}{2B}=\frac{u_2^2}{\frac{n\tan(\beta_2-\gamma_2)}{30b_2\psi_2}+\frac{2nD_1\tan\gamma_1}{15\left(D_1^2-D_h^2\right)\psi_1}} \tag{7}$$

At this moment, the shaft power P has the maximum value. Therefore,

$$P_{max}=\frac{A^2}{4B}=\frac{\rho u_2^4}{\frac{200\rho\eta_m\tan(\beta_2-\gamma_2)}{3b_2\psi_2}+\frac{800\eta_m nD_1\tan\gamma_1}{3\left(D_1^2-D_h^2\right)\psi_1}} \tag{8}$$

The above equations can also be used in the analysis of SPCPs under two different operating conditions: series condition and parallel condition. Eqs. (7) and (8) can be applied to any of the two conditions. Given that the two impellers are the same, the shaft powers of the two impellers have the same maximum value when the local flow rate is equal to Q_t'. Therefore, when SPCPs are under the series operating condition, the local flow rate Q_{St}' is equal to Q_t', and the value of P_{Smax} is twice that of P_{max}; when the SPCP is under the parallel operating conditions, the local flow rate Q_{Pt}' is twice that of Q_t', and the value of P_{Pmax} is also twice that of P_{max}.

Eq. (8) shows that the maximum shaft power is related to some parameters, including the flow deviation angle, γ_i, the inlet and exit excretion coefficient of blades, ψ_1 and ψ_2, the inlet and exit impeller diameter, D_1 and D_2, and the rotational speed, n. Although the geometric dimensions of the impeller combine well with the volute, P_{max} is only related to γ_i. Moreover, the impellers of SSMPs are designed using multi-factor orthogonal experimental methods. Consequently, the trend of the shaft power curves is only changed by γ_i of SPCPs.

The flow deviation angle, γ_i, is adopted to evaluate the non-uniform flow phenomenon in SPCPs and can be computed from the relation at the impeller inlet sections:

$$\gamma_1=90°-\arctan\left|u_{ti}/u_{ai}\right| \tag{9}$$

where u_{ti} is the tangential velocity at the inlet cross-section of the impeller, and u_{ai} is the radial velocity at the inlet cross-section of the impeller.

At the impeller exit sections, the non-uniform flow phenomenon in SPCPs can be obtained as follows:

$$\gamma_2=\beta_2-\arccos\left|V_X/\bar{V}\right| \tag{10}$$

where V_x is the velocity of the X axis direction, V_Y is the velocity of the Y axis direction, and $\bar{V}$ can be written as $\sqrt{V_X^2+V_Y^2}$.

3.3 Numerical scheme and solution convergence

The 3D models of SPCPs are shown in Fig. 3 a. The two different 3D models of the inlet passages under the series operating condition and the parallel operating condition are presented in Figs. 3 b and 3 c, respectively.

Validation of the independence of mesh density at a nominal flow rate of SSMPs is conducted. The grids for the experiments are listed in Table I.

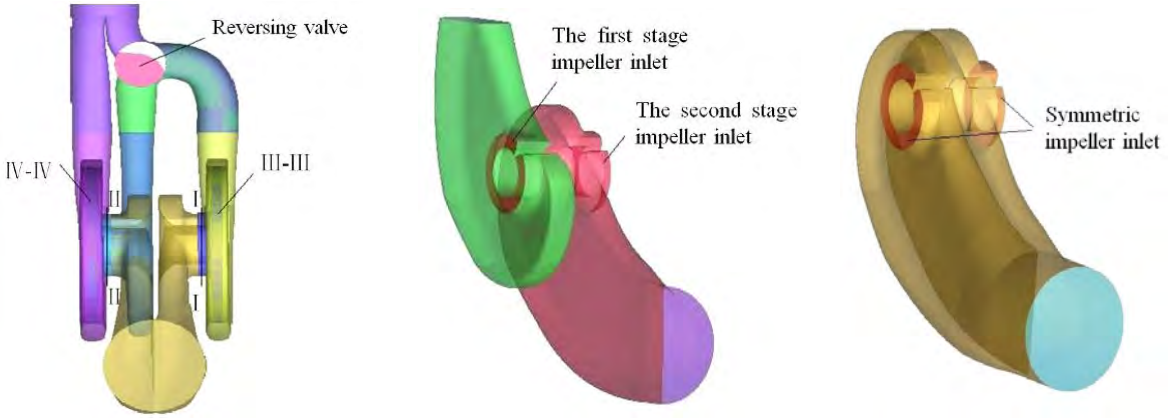

a) Three-dimensional model of SPCPs

b) Inlet passage of the series condition

c) Inlet passage of the parallel condition

Figure 3: Numerical models.

The full 3D unstructured grids are adopted to mesh, as shown in Fig. 4, to ensure the orthogonality and smooth variation of the cells in the computational domain. The refined mesh is set in the domain near the blades. The non-dimensional wall distances are targeted as $y+\leq 40$ in the near-wall region. Therefore, the y+ of all the walls, including the shroud wall and hub, is less than 40. The mesh can be smoothened with respect to a particular quality criterion and a specified number of iterations to achieve a given quality level. The number of iterations is five, and the quality level is greater than 3.5. A mesh containing tetras, pyramids, prisms, and triangular and quad surface elements can be smoothened. The computational model employs a mesh with 1,532,591 elements for the simulation. The increment of the head of the pump is about 0.34 %. The total number of grids of the impeller and volute of the SSMP is the same as that in Mesh 4, as listed in Table I. When the pump is SSMP, the total number of grid elements of the impeller and volute is the same as that in Mesh 4 (see Table I).

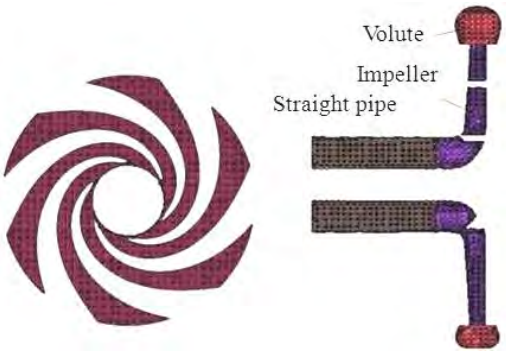

Figure 4: Impeller and assembly of mesh.

Table I: The independence validation of mesh density for SSMPs.

Item	Mesh 1	Mesh 2	Mesh 3	Mesh 4
Impeller	465,310	493,893	512,138	629,333
Volute	322,730	415,137	422,719	432,907
Whole box	1,013,925	1,298,543	1,495,208	1,532,591
Head/m	74.17	75.44	76.32	76.58

The standard k-ε model is appropriate to analyse the turbulence under the design condition, which is widely used in the hydraulic performance prediction of centrifugal pumps. However, the standard k-ε model fails to predict the hydraulic performance of the pumps under the off-design condition, which can be coupled with the re-normalization group (RNG) k-ε turbulence

model. Thus, the RNG k-ε turbulence model is employed to simulate the internal flow field of the pumps in this paper.

In the commercial software Fluent, the finite volume method is used for the discretization of the equations. The pressure-based solvers, pressure-implicit, and SIMPLE are used to simulate the pressure correction. The convective term and the diffusion term are represented using the second-order upwind scheme. Time discretization is achieved using the first-order fully implicit scheme. An algebraic multigrid solver is adopted to solve the equations. Maximum residuals are set to 10^{-5}, and the mass flow value and static pressure value at the pump inlet and exit are monitored. When the overall imbalance of the four monitors is less than 0.1 % or when the maximum residuals are reached, the simulation is considered steady and convergent.

For a steady flow, the simulation is conducted using the multi-reference frame technique, in which the impeller is situated in the rotating reference frame and the volute is situated in the fixed reference frame. The grids with different domains are connected through the interfaces. The mass flow rate is specified at the pump inlet, and the pressure exit boundary is used at the pump exit. The average turbulence intensity is considered at 5 %, which is a completely empirical value because the inflow to the pump from a high suction reservoir requires a much rectified time. Smooth nonslip wall conditions are set for all physical surfaces, except for the interfaces between the different parts.

3.4 Experimental measurement for pumps

An enclosed experimental setup is established to investigate the characteristics of SPCPs, as shown in Fig. 5. The experiments are conducted according to the Chinese Grade 1 precision (GB3216-2005) and the international grade 1 precision (ISO9906-1999). The inlet pressure and exit pressure of SPCPs are accurately measured at about ±0.1 % with pressure sensors, the flow rate is accurately measured at about ±0.1 % with an electromagnetic flow meter, and the electrical power input is measured with a three-phase torque meter. The overall measurement uncertainty is calculated from the square root of the sum of the squares of the systematic and random uncertainties [17], and the calculated results of the expanded uncertainty of efficiency is 0.5 %. The performance of the original pump at multi-flow rates is tested by experiments.

The total efficiency of the pump can be obtained as:

$$\eta = \frac{Q(p_{out} - p_{in})}{P_{\text{shaft}}} \tag{11}$$

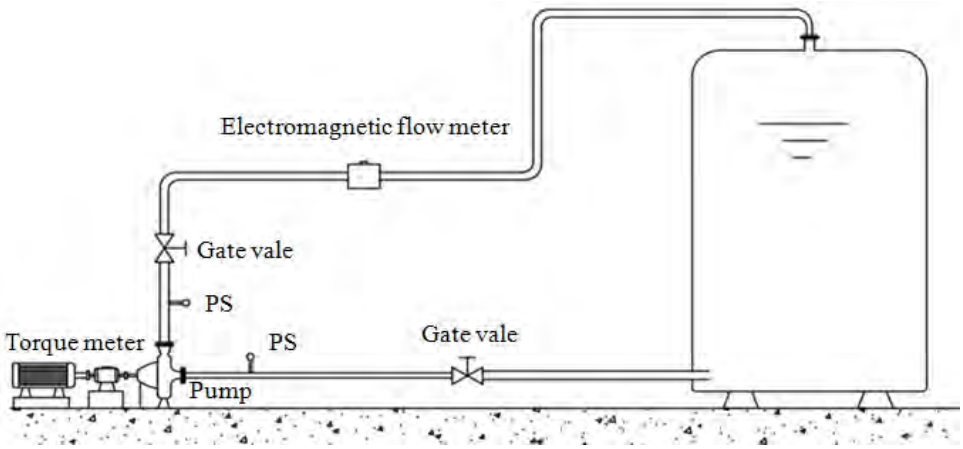

Figure 5: Experimental set-up.

In Eq. (11), p_{out} and p_{in} are the testing pressures at the exit and inlet of the pump, respectively. P_{shaft} is the input electrical shaft power measured using a three-phase torque

meter. The above parameters can be measured using the testing sensor. Therefore, the total efficiency of the pump can be calculated directly from Eq. (11). The relationship among the parameters is shown by the curves in the picture.

4. SIMULATION ANALYSIS AND DISCUSSION

The external characteristic curves of SPCP are shown in Fig. 6. The simulation results are in good agreement with the experimental results. The errors in the head, power, and efficiency of SPCP under the serial operating conditions are 3.78 %, 4.15 %, and 3.55 %, and those in the head, power, and efficiency of SPCP under the parallel operating conditions are 2.87 %, 3.51 %, and 5.36 %, respectively. The computational head and efficiency curves are slightly higher than the experimental curves, and the computational power curves are slightly lower than the experimental curves because of the neglect of volume loss and mechanical friction loss in the calculation [18]. Computational accuracy can fully meet the requirements in the engineering application, and the CFD can accurately predict the internal flow pattern of the pumps.

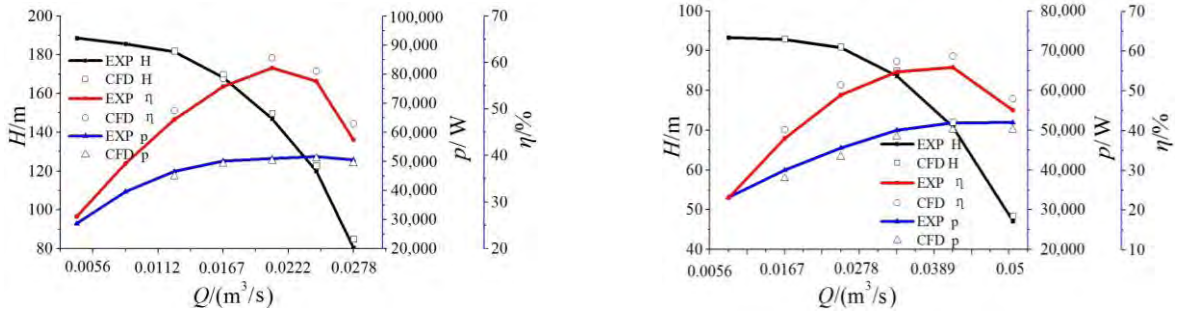

a) Series operating conditions of SPCPs b) Parallel operating conditions of SPCPs

Figure 6: Comparison between experimental and numerical results of pumps.

4.1 Non-uniform flow analysis of SPCPs

The distributions of the non-uniform flow deviation angle γ_i at the inlet and exit of the impeller of SPCPs at the designed flow rate under the serial operating condition are shown in Fig. 7, and the cross-section is presented in Fig. 1 c. The cross-section I-I is a free pressure inlet in the first-stage impeller, the cross-section II-II is a pressure inlet in the second-stage impeller, and the cross-section III-III and cross-section IV-IV are the pressure outlets located in the first-stage impeller and the second-stage impeller, respectively. The value of γ_1 increases before the flow arrives at the second-stage impeller inlet because of the influence of the exit flow non-uniformity of the first-stage impeller. Comparing the values of γ_2 between cross-section III-III and cross-section IV-IV, the magnitude of γ_2 at the back impeller exit is slightly larger than that of the front impeller exit, thus indicating that the flow-deviation phenomenon at the second-stage impeller exit is much evident.

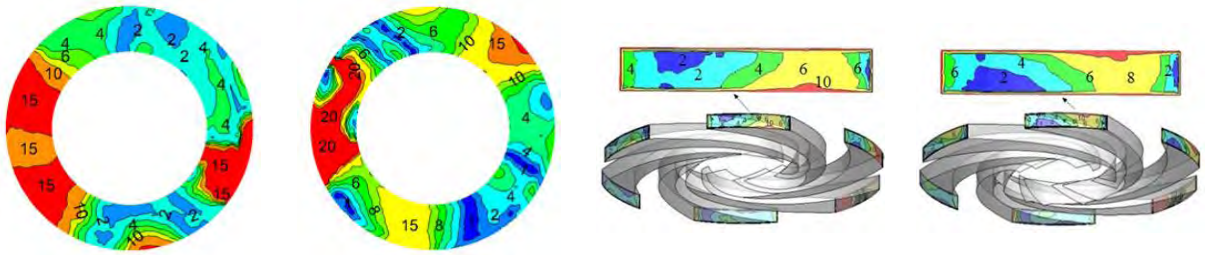

a) Cross section I-I b) Cross section II-II c) Cross section III-III d) Cross section IV-IV

Figure 7: The γ_i distributions on different sections of SPCPs under serial operating condition, unit (°).

The distributions of the flow deviation angle γ_i at the inlet and exit of the impeller of SPCPs at the designed flow rate under the parallel operating condition are shown in Fig. 8. The suction conditions of the cross-section I-I are the same as those of the cross-section II-II. The distributions of γ_1 of the cross-section I-I and the cross-section II-II are symmetrical and slightly different because of the influence of the different exit constructions. The distributions of γ_2 of the cross-section III-III and the cross-section IV-IV are also symmetrical. Moreover, the distribution pattern is similar to that of the first-stage impeller, in which the flow-deviation phenomenon near the suction side of the impeller exit is evident.

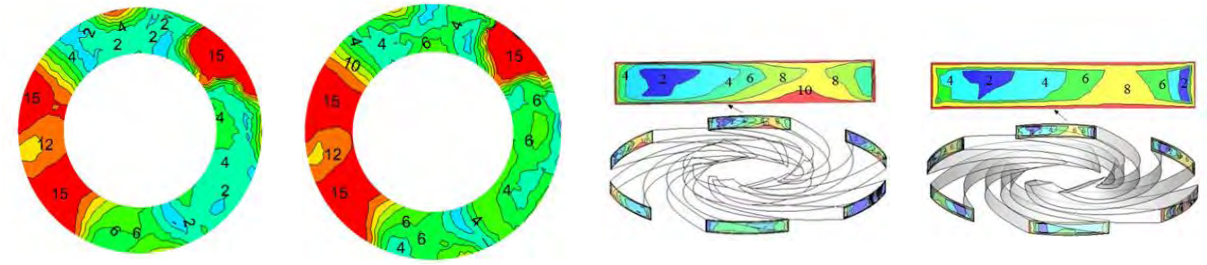

a) Cross section I-I b) Cross section II-II c) Cross section III-III d) Cross section IV-IV

Figure 8: The γ_i distributions on different sections of SPCPs under parallel operating condition, unit (°).

4.2 Analysis on non-overload characteristics

To simplify the calculations of the 3D turbulence flows, the flow deviation angles of the impeller inlet and exit under different operating conditions are averaged in this section. These deviation angles can convert complex 3D problems into simple 1D problems to obtain their solutions. At present, this method is widely used in hydraulic machinery. For example, when evaluating the hydraulic performance of the inlet passage in large pumping stations, the two parameters of axial velocity distribution and velocity-weighted average swirl angle are introduced, and the complex 3D turbulent flows are transformed into a simple 1D flow. In this paper, this method is used, and the calculated results are substituted into Eqs. (7) and (8) in section 3.2 to obtain the non-overload characteristics under different operating conditions.

The effects of non-uniformity on the non-overload hydraulic performance of SPCPs are listed in Table II. Where $\bar{\gamma}_1$ and $\bar{\gamma}_2$ are the weighted average of the γ_1 and γ_2 in different sections, respectively. The CFD simulation is in good agreement with the experimental results when the non-uniform flow deviation angles are considered. When $\bar{\gamma}_1 = 12.18°$ and $\bar{\gamma}_2 = 5.27°$, the calculated error values of Q'_{St} and P_{Smax} under the series operating conditions are larger than the experimental values, which are 1.30 % and 4.89 %, respectively. When $\bar{\gamma}_1 = 10.92°$ and $\bar{\gamma}_2 = 4.15°$, the calculated error values of Q'_{Pt} and P_{Pmax} under the parallel operating conditions are larger than the experimental values, which are 1.32 % and 4.15 %, respectively. Consequently, the flow deviation angle plays a significant role in the non-overload characteristics of SPCPs.

In Table II, when the SPCPs are under the serial operating condition, the value $\bar{\gamma}_1$ of the second-stage impeller inlet becomes large, i.e., $\bar{\gamma}_1 = 5.27°$. Satisfying the non-overload characteristics is easy. When $Q'_{St} = 0.0246$ m³/s, the pump reaches the maximum value of power under the series operating condition; when $Q'_{Pt} = 0.0502$ m³/s, the pump reaches the maximum value of power under the parallel operating condition. Moreover, because the flow rate under the parallel operating conditions is twice that of SSMPs, the maximum value of the power appears only when $Q'_t = 0.0251$ m³/s. When a distinct non-uniform flow phenomenon exists in the impeller inlet cross-section and exit cross-section, the head of the pump is reduced and a premature arrival at the maximum value on the power curve occurs. The head of the pump rapidly decreases when the distinct non-uniform flow phenomenon appears in the

impeller inlet cross-section and exit cross-section, thus causing the power curve to reach the maximum point. Therefore, the larger the $\bar{\gamma}_i$ is, the earlier the possible appearance of the non-overload characteristics of the pump. In addition, the pump is more likely to achieve the non-overload characteristics with a larger $\bar{\gamma}_i$.

Table II: Effect of non-uniformity on the non-overload characteristics of SPCPs.

SPCPs	Parameters	$\bar{\gamma}_i$ (°)		Q'_{St} or Q'_{Pt} (m³/s)			P_{Smax} or P_{Pmax} (W)		
	Cross section	Uni.	Non-Uni.	Uni.	Non-Uni.	EXP.	Uni.	Non-Uni.	EXP.
Series operating condition	I-I	0	12.18	0.0370	0.0246	0.0249	37.510	48.980	51.500
	III-III	0	5.27						
	Error (%)	—	—	50.34	1.30	—	45.67	4.89	—
Parallel operating condition	I-I, II-II	0	10.92	0.0740	0.0528	0.0503	75.020	54.610	53.900
	III-III, IV-IV	0	4.15						
	Error (%)	—	—	47.26	5.15	—	39.18	1.32	—

5. CONCLUSIONS

To prevent SPCPs from burning out the motor when working overload, the mechanism of overload must be analysed to consider the non-uniform flow. In the present study, the RNG k–ε turbulence model provided by the FLUENT software is applied to examine the flow field of the 3D flow deviation angles used in the non-overload characteristics of SPCPs. The following conclusions can be drawn from this study:

(1) In the non-overload characteristics, when the internal flow of the pump is uniform, the calculated error values under the non-overload operating conditions are larger than the experimental values. However, when the internal flow of the pump is non-uniform, the calculated error value of the local flow rate and shaft powers under the non-overload operating conditions are smaller than the experimental values. Moreover, the theoretical method and the numerical simulation used in this paper can accurately calculate the non-overload characteristics of SPCPs.

(2) The analysis of the effect of the flow deviation angle on the non-overload characteristics of pumps under different operating conditions shows that the pumps can likely achieve the non-overload characteristics at a large flow deviation angle at the impeller inlet. That is, the pumps can more likely achieve the non-overload characteristics under the serial operating condition than under the parallel operating condition.

In the design of SPCPs, two methods should be adopted to achieve the non-overload hydraulic performance. The first method is to place a pre-swirling plate at each inlet of the two impellers and to retain the exit angle of the plate with the flow angle to decrease the rapid increase in the head. The second method is the use of the multistage impeller series to enhance the flow non-uniformity at the impeller inlet and exit. These methods and the corresponding test verification must be considered in future related studies.

ACKNOWLEDGEMENTS

This study was supported by the Fundamental Research Funds for the Central Universities (Grant no. JZ2015HGBZ0469, JZ2015HGBZ0128 and JD2016JGPY0006).

REFERENCES

[1] Ma, S.-H.; Yu, D.-G.; Xie, J.-H.; Jiang, Q.; Wang, X.-D.; Wang, G.-X. (2002). Development of a new-type serial-parallel two-stage centrifugal pump, *Ship Engineering*, Vol. 25, No. 6, 38-41, doi:10.3969/j.issn.1000-6982.2002.06.009

[2] Joshi, S.; Gordon, A.; Holloway, L.; Chang, L. (2005). Selecting a high specific speed pump for low head hydro-electric power generation, *Canadian Conference on Electrical and Computer Engineering*, 603-606, doi:10.1109/CCECE.2005.1557003

[3] Chen, B.; Zhang, H.; Shi, W.; Zhang, D.; Xu, Y. (2012). Numerical calculation and experiment of non-overload low specific speed sewage pump with super-thick blades, *Transactions of the Chinese Society for Agricultural Machinery*, Vol. 43, No. 5, 74-78, doi:10.6041/j.issn.1000-1298.2012.05.013

[4] Su, X.-Z.; Yang, C.-X.; Li, Y-.B.; Li, Q. (2014). Effect of impeller inlet condition on non-overload performance of serial-parallel centrifugal pump, *Transactions of the Chinese Society of Agricultural Engineering*, Vol. 30, No. 13, 60-67, doi:10.3969/j.issn.1002-6819.2014.13.008

[5] Ma, Y.; Ma, Z.-Q.; Zhang, S.-C. (2015). A novel design method for impeller of medium specific speed non-overload multistage centrifugal pumps, *Journal of Shanghai Jiaotong University*, Vol. 49, No. 5, 695-701, doi:10.16183/j.cnki.jsjtu.2015.05.020

[6] Shi, W.-D.; Li, H.; Lu, W.-G.; Dai, J.; Li, X. (2013). Effect of prewhirl flow on non-overload performance of low-specific-speed centrifugal pumps, *Transactions of the Chinese Society for Agricultural Machinery*, Vol. 44, No. 5, 50-54, doi:10.6041/j.issn.1000-1298.2013.05.010

[7] Yu, P.; Sun, W.; Yang, Z. (2002). Design and research of marine submersible series multiple centrifugal pump, *Mechanical and Electrical Equipment*, Vol. 17, No. 4, 1-6

[8] Li, Y. Study on the flow and vibration characteristics of marine serial-parallel centrifugal pump, from *http://d.wanfangdata.com.cn/Thesis/Y2748345*, accessed on 30-07-2015

[9] Li, Y.; Shi, W.; Han, X. (2015). Effects of pump hydraulic structure on vibration characteristics of series-parallel centrifugal pump, *Journal of Drainage and Irrigation Machinery Engineering*, Vol. 33, No. 9, 744-749, doi:10.3969/j.issn.1674-8530.14.0173

[10] Anderson, H. H. (1995). *Centrifugal Pumps and Allied Machinery*, 4th ed., Elsevier Science, Oxford

[11] Anderson, H. H. (1980). Prediction of head, quantity and efficiency in pumps – the area ratio principle, *Proceedings of the 22nd Annual Fluids Engineering Conference*, 9-13

[12] Yuan, S. Q. (1993). Research on non-overload low specific speed centrifugal pump for agricultural use, *Transactions of the Chinese Society of Agricultural Engineering*, Vol. 9, No. 3, 78-84

[13] Zhang, J.-F.; Zhang, Y.-L.; Yuan, S.-Q.; Mao, J.-Y. (2014). Optimization design of high-efficiency non-overload on a low-specific speed centrifugal pump, *Transactions of the Chinese Society for Agricultural Machinery*, Vol. 45, No. 5, 91-95, doi:10.6041/j.issn.1000-1298.2014.05.014

[14] Feng, J.; Benra, F.-K.; Dohmen, H. J. (2010). Investigation of periodically unsteady flow in a radial pump by CFD simulations and LDV measurements, *Journal of Turbomachinery*, Vol. 133, No. 1, 11 pages, doi:10.1115/1.4000486

[15] Zhang, J.-F.; Yuan, Y.; Yuan, S.-Q.; Lu, W.-G.; Yuan, J.-P. (2011). Experimental studies on the optimization design of a low specific speed centrifugal pump, *Proceedings of the 23rd Symposium on Fluid Machinery*, 561-569, doi:10.1115/AJK2011-22005

[16] Hu, B.; Yuan, S. Q.; Lu, W. G.; Yuan, J. P; Li, L. (2012). Optimal design of a non-overload centrifugal pump, *Advanced Material Research*, Vols. 468-471, 2357-2363, doi:10.4028/www.scientific.net/AMR.468-471.2357

[17] Feng, H. D.; Xu, L.; Xu, R. P.; Wu, L. J.; Shi, X. H.; Yan, J. D.; Wang, T. Y. (2004). Uncertainty analysis using the thermodynamic method of pump efficiency testing, *Proceedings of the Institution of Mechanical Engineers, Part C: Journal of Mechanical Engineering Science*, Vol. 218, No. 5, 543-555, doi:10.1243/095440604323052328

[18] Tamm, A.; Ludwig, G.; Stoffel, B. (2001). Numerical, experimental and theoretical analysis of the individual efficiencies of a centrifugal pump, *Proceedings of ASME Fluids Engineering Division Summer Meeting 2001*, 23-34